STUDIES OF ENHANCED FIELD EMISSION RELEVANT TO HIGH FIELD SUPERCONDUCTING RADIO FREQUENCY DEVICES

by

Marija D. RADMILOVIĆ-RADJENOVIĆ [*]***, Željka D. NIKITOVIĆ, and Branislav M. RADJENOVIĆ***

Institute of Physics, University of Belgrade, Belgrade, Serbia

Scientific paper
https://doi.org/10.2298/NTRP210121007R

Surface roughness represents the measure of the irregularities on the surface contributing to the local field enhancement. The traditional Fowler-Nordheim equation established for perfectly planar surfaces is not suitable for describing emission from rough surfaces. Instead, it is more appropriate to use the equation that accounts for the field enhancement factor describing the effect of the surface morphology. In superconducting radio frequency cavities, field emission may occur in the irises while the tips on the cavity surface may act as an emitter leading to the high electric field. For this study, calculations for hemispherical, cylindrical, and conical tips have been performed using a Multiphysics software package COMSOL. The focus was put on the dependence of the field enhancement factor on the shape and the radius of the protrusions. The electric field strength and the current density increase with increasing the root mean square average of the profile heights due to field enhancement at the cavity irises. The lowest value of the electric field has been achieved for the hemisphere. The calculated values for the field enhancement factors are consistent with the data from the literature, in which case the protrusion may represent a small local bump on the surface of a superconducting cavity. Based on the fit of the results, presented here, the relation between the enhancement factor and the radius has been suggested. The accurate estimation of the field emission may play a crucial role in the design of accelerators and other technological applications with requirements of extremely high precision.

Key words: accelerator, cavity, breakdown, COMSOL

INTRODUCTION

The strong electric field at the irregularities on the cavity surface enhances electron emission leading to the field emission (FE) effect. Electron emission from the sharp tips due to FE is recognized as one of the most severe constraints in high-gradient accelerator structures [1-6]. The main cause of FE in superconducting cavities is particulate contamination. Scratches or other geometrical defects on the cavity surface operate as field emitters creating a field emitted current and reducing the quality factor [7]. Superconducting cavities are much more sensitive to FE as additional dissipation of radio frequency (RF) power due to the electron loading of the cavity may cause significant and undesirable degradation of the quality factor [8]. Thus, there is significant interest in understanding the origin of FE in cavities with applications in superconducting radio frequency (SRF) cavity design, construction, and operation.

The FE represents the tunneling of electrons through a barrier in the presence of a strong electric field mathematically expressed via Fowler-Nordheim (FN) equation [9, 10]. In accelerators, FE is responsible for unwanted effects such as absorption of RF power, dark current, and possible breakdown. The traditional FN theory is shown to be a restricted case of a generalized FN type equation in the limit of a perfectly at the surface of a material with parabolic dispersion [11, 12]. When a simple quantitative test for lack of FE has been conducted by applying the original FN equation to the data available in the literature, almost half the examined data failed this test [13].

To solve this problem, many analytical or semi-analytical works that address emissions from specific geometry emitters have been performed [14, 15]. Some of them treat emission with no equation applicable to arbitrarily sharp nanoscopic tips [16]. Later, the sphere on a cone model has been developed containing functions of two variables that have to be evaluated numerically and thus are not easy to use [17]. Zuber *et al*. [18] recognized the emission from

* Corresponding author; e-mail: marija@ipb.ac.rs

hyperboloid surface element as FN type. From the first principles, Kyritsakis and Xanthakis [19] derived a generalized FN equation that involves the curvature of a nanoscopic emitter. Geometrical effects can also be considered by the field enhancement factor defined as the ratio of the local electric field over the applied field. In general, the field enhancement causes fields about sharp points to be large.

In this paper, the enhancement of the field generated around hemispherical, cylindrical, and conical protrusions has been studied using the software package COMSOL Multiphysics [20]. In COMSOL rough surface is characterized by using a sum of trigonometric functions similar to a Fourier series expansion. The role of the surface roughness on the enhancement of the electric field and the current density has been analyzed. The enhancement factor for hemispherical, cylindrical, and conical protrusions has been estimated and compared. Based on the fit of the calculation results relationship between the enhancement factor, β, and the radius, r, has been suggested.

FIELD ENHANCEMENT

The FE emission from the surface of a material is the extraction of electrons from a surface by tunneling through the surface potential barrier. The FE current density, j_{FE}, is given by the expression [21]

$$j_{\mathrm{FE}} = e\int_0^{\infty} n(\delta)D(\delta,E)\mathrm{d}\delta \tag{1}$$

where e is the electron charge, D – the transmission coefficient, δ – the fraction of the electron's energy related to the component of momentum normal to the surface, and E – the electric field. Originally, the FN equation has been established for cold flat surfaces, but in practice, no metal surface in an accelerator cavity is perfectly flat.

Geometrical effects in the FN equation can be introduced by the field enhancement factor defined as the ratio of an electric field in the presence of a protrusion and the field in the absence of the protrusion. The expression for the electron current density, j_{FE}, has the form [22]

$$j_{\mathrm{FE}} = \frac{1.54\beta^2E^2}{\phi}\mathrm{e}^{10.41\phi^{-1/2}}\mathrm{e}^{[-6.53\,\phi^{3/2}/(\beta E)]} \tag{2}$$

where E is the electric field, ϕ – the material work function (expressed in eV), and β – the field enhancement factor. Figure 1 contains calculated values of the field enhancement factor for several geometries (a sphere above a plane, a cylinder topped by a semi-sphere, and an ellipsoid) characterized by the height, h, radius, ρ and $\rho = \kappa^2/h$ (for ellipsoid) [23]. An emission source with a greater field enhancement factor can produce a larger field and enhance the electron emission. As can be seen from fig. 1, the largest

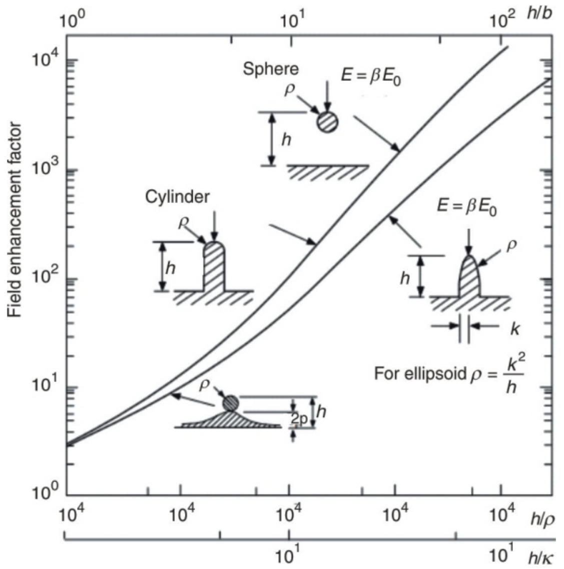

Figure 1. Calculated values for the field enhancement factor *vs.* h/ρ (or h/κ) for various microprotrusion geometries [23]

electric field strength corresponds to a sphere above a plane, while the smallest to a semi-sphere.

The enhancement is a dimensionless ratio of fields and is a function of the geometry

$$\beta = \frac{E}{E_0} = -\frac{1}{E_0}\partial_z V(z,\rho)\big|_{z=h_0,\rho=0} = a\partial_z u(z,\rho)\big|_{z=h_0,\rho=0} \tag{3}$$

where h_{a} is the height of the protrusion and $\partial_z u(z,\rho) = 1$ for the protrusion-free case *i. e.*, for $\delta = 0$.

In the case of the hemisphere on a plane, the system is characterized by the rotational symmetry about the z-axis and the potential can be expressed in terms of the Legendre polynomials [24].

$$V(r,\theta) = \sum_{i=0}^{\infty}\left(A_l r^l + \frac{B_l}{r^{l+1}}\right)P_l(\cos\theta) \tag{4}$$

Far away from the hemisphere, $r \to \infty$, $V(r,\theta) \to -E_{\mathrm{o}}z = -E_{\mathrm{o}}r\cos\theta$. Along the surface of the hemisphere, the enhancement factor is

$$\beta(\theta) = -\frac{1}{E_0}\partial_r V(r,\theta)\big|_{r=a} = 3\cos\theta \tag{5}$$

For a conical emitter in a background field E_{o}, such that the ellipsoid is defined by $\eta = \eta_{\mathrm{o}}$, and asymptotically, the potential is that of a constant background field [24]

$$\lim_{\eta\to\infty} V(\eta,\upsilon) = -E_0 z = -E_0 L\cosh\eta\cos\upsilon \tag{6}$$

where the angles $(\eta\ \upsilon)$ $A_{\mathrm{mn}}\cos(\mathbf{k}_{\mathrm{mn}}\ \mathbf{x} + \varphi)$ are related to the cylindrical co-ordinates (z, ρ) according to

$$\rho \quad L\sinh(\eta)\sin(\upsilon) \tag{7}$$

$$z \quad L\cosh(\eta)\cos(\upsilon) \tag{8}$$

where L is a length scale. For Poisson's equation $\;^{2}V = 0$, and using $V(\eta, \upsilon) = E_{o}L\, U(\eta)W(\upsilon)$ [24]

$$\frac{1}{U} \quad \frac{1}{\sinh\eta}\frac{\partial}{\partial\eta} \quad \sinh\eta\frac{\partial U}{\partial\eta}$$
$$\frac{1}{W} \quad \frac{1}{\sin\upsilon}\frac{\partial W}{\partial\upsilon} \quad \sin\upsilon\frac{\partial}{\partial\upsilon} \tag{9}$$

From the asymptotic behavior, $W = \cos\upsilon$, while $U(\eta) = -\cosh\eta + A_1Q_1(\cosh\eta)$, where

$$Q_l(\cos\eta) \quad \frac{\cosh\eta}{2}\ln\frac{\cosh\eta \quad 1}{\cosh\eta \quad 1} \quad 1 \tag{10}$$

and A_1 is determined by the boundary condition that on the surface of the ellipsoid ($\eta = \eta_o$), the potential vanishes.

NUMERICAL METHOD

For this study, calculations were performed using the software package COMSOL based on a multi-component plasma fluid model solved by the finite element method [20]. The COMSOL Multiphysics represents an integrated software environment for creating physics-based models and simulation applications. In COMSOL Multiphysics surface roughness can be represented as a sum of trigonometric functions similar to a Fourier series expansion [25]. A rough surface $f(x, y)$ is composed of many elementary waves. Each constituent wave component can be expressed in the form [25]

$$A_{\rm mn}\cos(k_{\rm mn} \quad x \quad \varphi) \tag{11}$$

where φ is a phase angle and $A_{\rm mn}$ – the amplitude. For an entirely random surface, the phase angle, φ, lays in the interval 0 to π or $-\pi/2$ to $\pi/2$. The final surface is a sum over all wave components

$$f(x) \quad \underset{m,n}{} A_{\rm mn}\cos(k_{\rm mn} \quad x \quad \varphi) \tag{12}$$

To represent the rough surface that we generated for our calculations, we used the double sum

$$f(x, y) \quad \overset{M}{\underset{m \quad M}{}} \; \overset{N}{\underset{n \quad N}{}} a(m,n)\cos[2\pi(mx \quad ny) \quad \varphi(m,n)] \tag{13}$$

where x and y are spatial co-ordinates, m and n are spatial frequencies, a (m, n) are amplitudes, and $\varphi(m, n)$ are phase angles.

RESULTS

A rough surface topography contributes to the local field enhancement. Surface roughness represents the measure of the irregularities on the surface that can be characterized by the root mean square (RMS) height defined as the root mean square average of the profile heights over the evaluation length and labeled by Sq [26]. Figure 2 shows (a) 3-D, and (b) 2-D, images of the rough surface obtained by COMSOL Multiphysics. It can be noticed that these images are similar to atomic force microscope (AFM) images scanned over a surface area [27]. The RMS height was calculated to be 0.25 m. The locations of the high electric field produced by the sharp-edge features are painted red.

The effect of the RMS height on the electric field strength is illustrated in fig. 3. For the RMS height of 0.50 m, the electric field is more than two and around six times higher as compared to that for the RMS height of 0.25 m and 0.10 m, respectively. The higher RMS height leads to an emission increase due to local field enhancement at the sharp point protruding from the surface. For higher RMS height electric field may reach the threshold value for field emission.

Figure 4 displays the FN current density for the surface with various RMS heights. The current density is the lowest for flat surfaces (red circles), while for rough surfaces the current density increases with the RMS height increasing. The higher the RMS height, the higher the current density. Also, surface irregularities may become emitters if triggered by traces of immersed impurities. Figure 5 displays the enhancement factors calculated for fig. 5(a) RMS height of the protrusions of the surface and fig. 5(b) emitter areas. As expected, the enhancement factor increases with the RMS height increasing. The emission current of the various emitters can be determined from the modified FN equation [28]

$$\log\frac{I}{V^2} \quad \log a \quad 0.434 \quad \frac{b}{V},$$
$$a \quad 1.5 \;\; 10^{\;\;6}\frac{A}{\phi}\exp\frac{10.4}{\phi^{0.5}}, \; b \quad 6.44 \;\; 10^{7}\frac{\phi^{3/2}}{\beta} \tag{14}$$

where ϕ is the work function and A – the emitting area. The emission of electrons at low electric fields occurs from the sharp tip of the emitter resulting in a smaller emitting area with a greater field enhancement factor. At high electric fields, however, a large area of the emitter enhances electron emission, thereby reducing factor β. Assuming linearity of $\ln(I/V^2)$ with $1/V$ the slope and intercept on the FN plot is sufficient to determine field enhancement and emission area A.

Besides the height, the shape of the protrusion also affects the field enhancement factor. Calculated values of the enhancement factor of the field generated around are depicted in fig. 6(a) hemisphere, fig. 6(b) cylinder, and fig. 6(c) cone. The electric fields formed

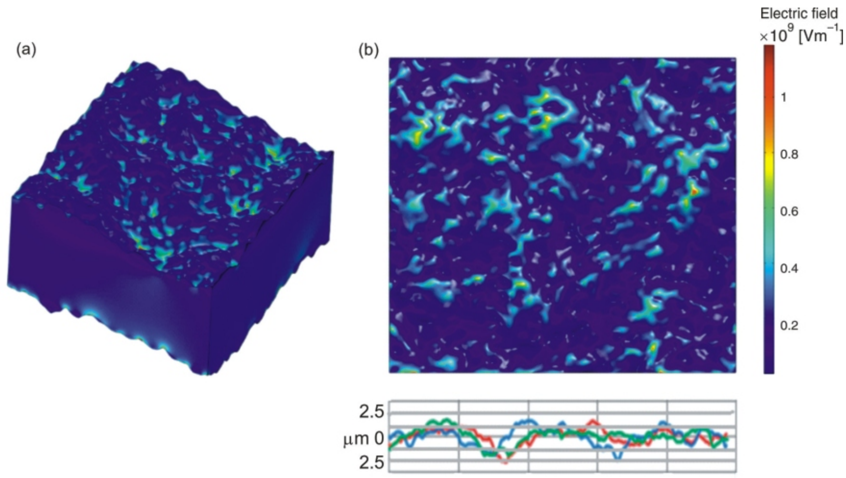

Figure 2. (a) 3-D and (b) 2-D images of rough surfaces characterized by the RMS height of 0.25 m

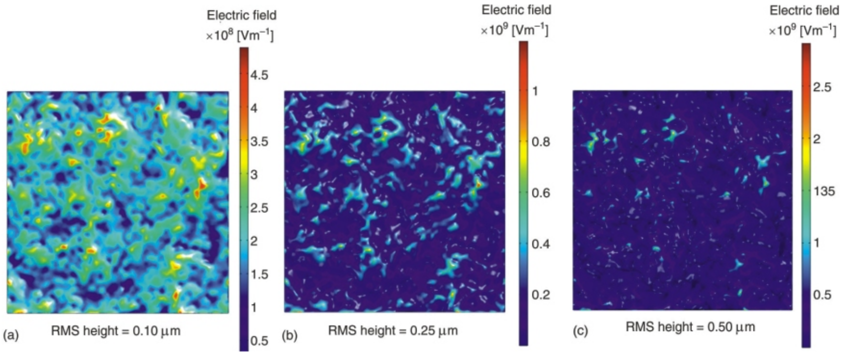

Figure 3. The electric field generated at the rough surface characterized by the RMS height: (a) 0.10 µm, (b) 0.25 µm, and (c) 0.50 µm

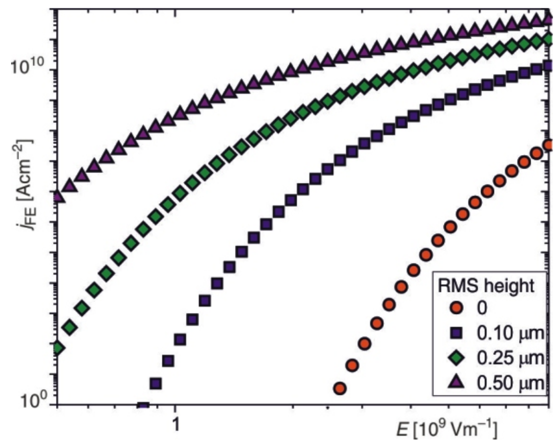

Figure 4. The Fowler-Nordheim current density for surfaces with the RMS height of 0 m (circles), 0.10 µm (squares), 0.25 µm (diamonds), and 0.50 µm (up triangles)

around conical and cylindrical tips are similar and higher than those around the hemisphere conforming to the calculated values of the enhancement factor shown in fig. 1.

It is shown that the radius plays a key role in the field enhancement. The dependence of the enhancement factor on the radius is represented in fig. 7(a) hemisphere, fig. 7(b) cylinder, and fig. 7(c) cone. The enhancement factor increases with the radius decreasing. It was reported in the literature that the relationship between the enhancement factor β and the radius r can

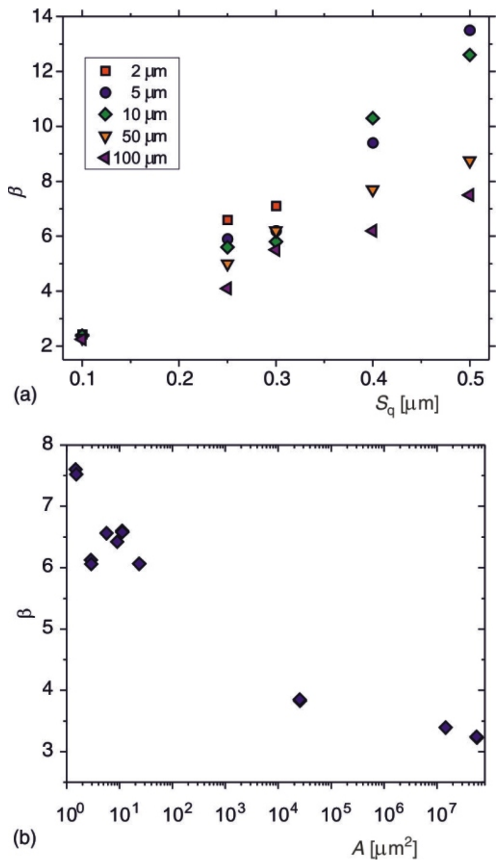

Figure 5. The dependence of the enhancement factor on: (a) RMS height *Sq* of the surface roughness and (b) emitter area *A*

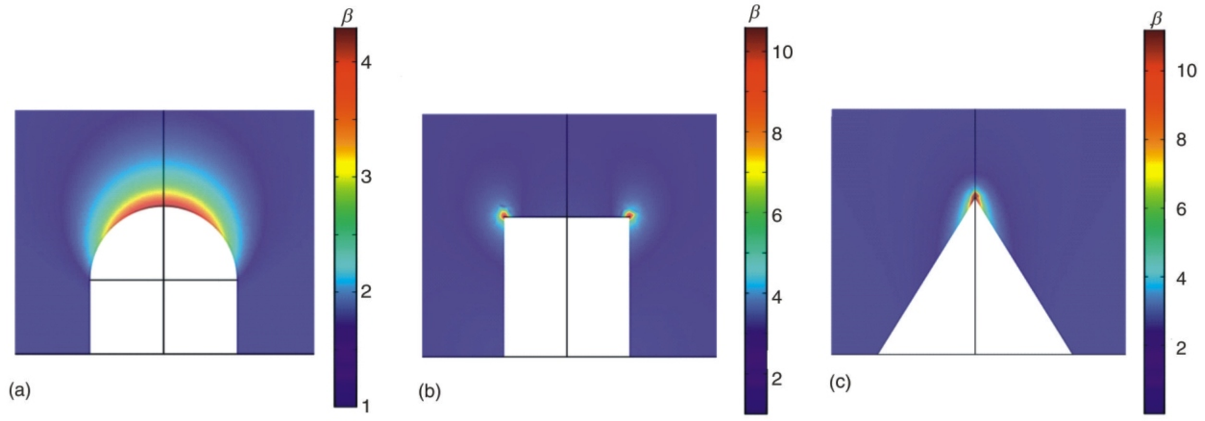

Figure 6. The calculated enhancement factor for (a) hemisphere, (b) cylinder, and (c) cone of the equal radius

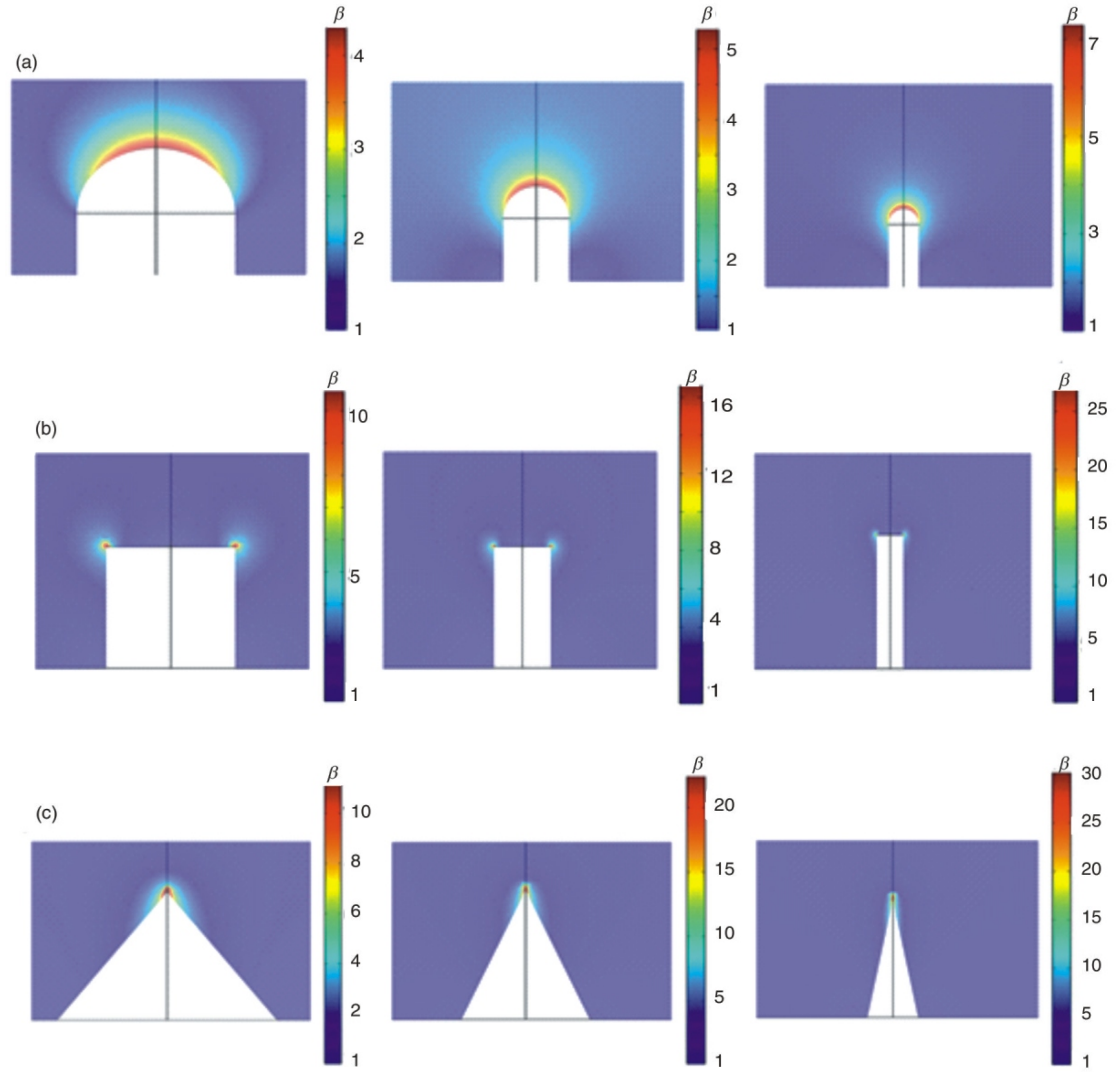

Figure 7. The effect of the radius on (a) hemispherical, (b) cylindrical, and (c) conical protrusions on the enhancement factor

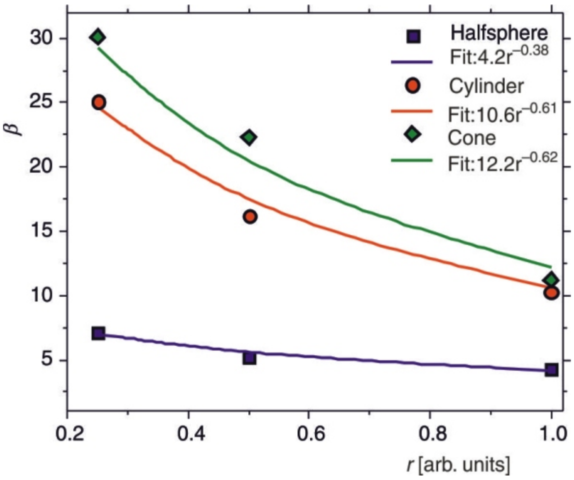

Figure 8. The dependence of the enhancement factor on the radius, *r*; calculation results and fits are presented by symbols and lines, respectively

be fitted approximately to $\beta \sim r^{-1/2}$ [29]. Based on our calculations shown in fig. 8 we may suggest that the enhancement factor, β, and the radius, r, can be fitted according to $\beta \sim ar^{-b}$ as plotted in fig. 8.

CONCLUSIONS

This study is related to the FE as one of the main constraints of the accelerating gradient in superconducting cavities remaining the dominant setback in cavity production. Calculations of the electric fields generated around hemispherical, cylindrical, and conical tips were carried out using COMSOL finite elements package. It is assumed that the rough surface is composed of many elementary waves. It was found that the RMS height of the protrusions affects the electric field and the current density. The higher the RMS height the higher field enhancement at the protrusion. For the RMS height of 0.50 m, the electric field strength is six and two times higher than those for 0.10 m and 0.25 m, respectively. The field enhancement due to contaminants and defects on the surface has been also estimated. At low electric fields, electron emission occurs from the sharp tip resulting in a smaller emitting area with a greater field enhancement factor. At high electric fields, however, the emitter area is large, while the enhancement factor is reduced. From our calculations, we estimated the enhancement factor of around 4 for the hemisphere, and around 11 and 12 for the cylindrical and the cone tips, respectively. Tips on the cavity surface may act as an emitter leading to the high electric field and thereby enhanced FE. With decreasing the radius of the protrusion, the enhancement factor increases. Based on the fit of the obtained results, the relation between the enhancement factor and the radius has been suggested. Results, presented here, could be useful to reduce FE in SRF cavities to reach higher accelerating gradients for future particle accelerators.

AUTHORS' CONTRIBUTIONS

The manuscript was written by M. D. Radmilović-Radjenović, and B. M. Radjenović. Simulations were conducted by M. D. Radmilović-Radjenović, Ž. D. Nikitović, and B. M. Radjenović. The figures were prepared by M. Radmilović-Radjenović and Ž. D. Nikitović.

REFERENCES

[1] Padamsee, H., RF Superconductivity: Science, Technology and Applications, Wiley-VCH Verlag GmbH & Co. KGaA, Weinheim, Germany, 2009
[2] Gurevich, A., Superconducting Radio-Frequency Fundamentals for Particle Accelerators, *Reviews of Accelerator Science and Technology, 5* (2012), pp. 119-146
[3] Kneisel, P., *et al.*, Review of Ingot Niobium as a Material for Superconducting Radiofrequency Accelerating Cavities, *Nucl. Instrum. Methods Phys. Res., Sect., A 774* (2015), pp. 133-150
[4] Ciovati, G., *et al.*, Superconducting Radio-frequency Cavities Made from Medium and Low-Purity Niobium Ingots, *Supercond. Sci. Technol., 29* (2016), 6, pp. 064002
[5] Posen, S., Hall, D. L., Nb3Sn Superconducting Radiofrequency Cavities: Fabrication, Results, Properties, and Prospects, *Supercond. Sci. Technol., 30* (2017), 3, pp. 033004
[6] Echevarria, P., *et al.*, Superconducting radio-Frequency Virtual Cavity for Control Algorithms Debugging, *Review of Scientific Instruments, 89* (2018), 8, pp. 084706
[7] Vogt, J. M., *et al.*, High-Q Operation of SRF Cavities: The Potential Impact of Thermo Currents on the RF Surface Resistance, *Physical Review Special Topics-Accelerators and Beams,18* (2015), 4, pp. 042001
[8] Romanenko, A., Schuster, D. I., Understanding Quality Factor Degradation in Superconducting Niobium Cavities at Low Microwave Field Amplitudes, *Phys. Rev. Lett., 119* (2017), 12, pp. 264801
[9] Egorov, N., Sheshin, E., Field Emission Electronics, Springer International Publishing, St. Petersburg, Russia, 2017
[10] Radmilović-Radjenović, M., *et al.*, The Effect of the Enhanced Field Emission on the Characteristics of the Superconducting Radio Frequency Cavities, *Nucl Technol Radiat, 33* (2018), 4, pp. 341-346
[11] Liang, S. D., Quantum Tunneling and Field Electron Emission Theories, New Jersey, World Scientific Publishing, New Jersey, 2014
[12] Forbes, R. G., 2013 Development of a Simple Quantitative Test for Lack of Field Emission Orthodoxy, *Proc. R. Soc., A 469* (2013), 2, pp. 20130271
[13] Fursey, G. N., Glazanov, D. V., 1998 Deviations from the FowlerNordheim Theory and Peculiarities of Field Electron Emission from Small-Scale Objects, *J. Vac. Sci. Technol., B16* (1998), pp. 910-915
[14] Parveen, S., *et al.*, Fowler Nordheim Theory of Carbon Nanotube Based Field Emitters, *Physica B: Condensed Matter, 505* (2017), pp. 1-8
[15] Edgcombe, C. J., de Jonge, N. J., Deduction of Work Function of Carbon Nanotube Field Emitter by use of Curved-Surface Theory, *Phys., D 40* (2007), pp. 4123-4128
[16] Katkov, V. L., Osipov, V. A., Influence of Tip Geometry on the Field Emission Law from Axisymmetric and

Wall-Like Emitters, *Europhysics Letters, 89* (2010), 1, pp. 17002
[17] Edgcombe, C. J., Development of FowlerNordheim Theory for a Spherical Field Emitter, *Phys. Rev., B 72* (2008), 4, pp. 045420
[18] Zuber, J. D., *et al*., 2002 An Analytical Solution for Microtip Field Emission Current and Effective, Emission Area, *J. Appl. Phys., 91* (2002), 11, pp. 9379
[19] Kyritsakis, A., Xanthakis, J. P., 2015 Derivation of a Generalized Fowlernordheim Equation for Nanoscopic Field-Emitters, *Proc. R. Soc., A 471* (2015), 2, pp. 20140811
[20] ***, COMSOL Multiphysics, available at https://www.comsol.com/.
[21] Radmilović-Radjenović, M. D., Radjenović, B. M., Simulation Study of Direct Current Vacuum Breakdown and its Application to High-Gradient Accelerating Structures, *Nucl Technol Radiat, 35* (2020), 1, pp. 30-35
[22] Forbes, R. G., Field Emission: New Theory for the Derivation of Emission Area from a Fowler-Nordheim Plot, J*ournal of Vacuum Science & Technology B, Nanotechnology and Microelectronics: Materials, Processing, Measurement, and Phenomena, 17* (1999), pp. 526-533
[23] Rohrbach, F.,On Mechanisms That Lead to Very High Voltage Electric Spark Formation in a Vacuum for Measuring Breakdown Delay Time, (CERN 71-28, October 1971)
[24] Jensen, K. L., Introduction to the Physics of Electron Emission, John Wiley & Sons, New Jersey, 2018
[25] ***, How to Generate Random Surfaces in COMSOL Multiphysics, available at https://www.comsol.com/blogs/how-to-generate-random-surfaces-in-comsol-multiphysics/
[26] Tonietto, L., *et al*., New Method for Evaluating Surface Roughness Parameters Acquired by Laser Scanning, *Scientific Reports, 9* (2019), 10, pp. 15038
[27] Butt, H. J., *et al*., Force Measurements with the Atomic Force Microscope: Technique, Interpretation and Applications, *Surf. Sci. Rep., 59* (2005), pp. 1-152
[28] Nicolaescu, D., *et al*., Model Parameter Extraction for Nonlinear Fowler-Nordheim Field Emission Data, *Journal of Vacuum Science & Technology, B 21* (2003), pp. 550-1555
[29] Khan, S., *et al*., (2007) Field Emission Properties of Fe70Pt30 Catalysed Multiwalled Carbon Nanotubes, *Journal of Experimental Nanoscience, 2* (2007), pp. 215-228

Received on January 21, 2021
Accepted on April 2, 2021

Марија Д. РАДМИЛОВИЋ-РАЂЕНОВИЋ,
Жељка Д. НИКИТОВИЋ, Бранислав М. РАЂЕНОВИЋ

ПРОУЧАВАЊЕ ЕМИСИЈЕ УСЛЕД ЈАКОГ ПОЉА КОД СУПЕРПРОВОДНИХ РАДИОФРЕКВЕНЦИЈЕНИХ УРЕЂАЈА

Храпавост површине представља меру неправилности површине која може да допринесе појачању локалног поља. Традиционална Фаулер-Нордхајмова једначина успостављена за савршено равне површине није погодна за описивање емисије са храпавих неправилних површина. Уместо ње много је погодније користити једначину која укључује фактор појачања поља који укључује ефекте морфологије површина. Код суперпроводних радиофреквенцијених шупљина емисија услед јаког поља дешава се на отворима (ирисима) и избочине на површинама се могу сматрати емитерима који могу да емитују честице услед јаког поља. За ово проучавање, прорачуни за избочине полусферних, цилиндричних и конусних облика извршени су коришћењем софтверског пакета заснованог на методу коначних елемената. Фокусирали смо се на зависност фактора појачања од облика и радијуса избочина. Јачина електричног поља и густина струје расту са порастом средње квадратне висине профила на отворима шупљина. Израчунате вредности за фактор појачања у сагласности су са подацима из литературе. Фитујући добијене резултате, предложена је релација која повезује фактор појачања и радијус. Тачна процена ефеката услед јаког поља има веома важну улогу у дизајну акцелератора и других технолошких примена које захтевају веома високу прецизност.

Кључне речи: акцелератор, шупљина, хаваријско заустављање, COMSOL